HOSTED BY

ELSEVIER

Contents lists available at ScienceDirect

Saudi Pharmaceutical Journal

journal homepage: www.sciencedirect.com

Pharmacokinetics and tissue distribution of vigabatrin enantiomers in rats

Qiang Zheng [a,b,c], Shuai He [a,b,c], Song-Lin Xu [a,b,c], Meng-Die Ma [a,b,c], Min Fan [a,b,c], Jin-Fang Ge [a,b,c,*]

[a] School of Pharmacy, Anhui Medical University, Hefei, Anhui 230032, PR China
[b] Anhui Provincial Laboratory of Inflammatory and Immune Disease, Anhui Institute of Innovative Drugs, Hefei, Anhui 230032, PR China
[c] The Key Laboratory of Anti-inflammatory and Immune Medicine, Ministry of Education, Anhui Medical University, Hefei, Anhui 230032, PR China

ARTICLE INFO

Keywords:
Vigabatrin
Single enantiomer
Pharmacokinetics
Distribution

ABSTRACT

Purpose: To investigate the pharmacokinetics and tissue distribution of VGB racemate and its single enantiomers, and explore the potential of clinic development for single enantiomer S-VGB.

Methods: In the pharmacokinetics study, male Sprague-Dawley rats were gavaged with VGB racemate or its single enantiomers dosing 50, 100 or 200 mg/kg, and the blood samples were collected during 12 h at regular intervals. In the experiment of tissue distribution, VGB and its single enantiomers were administered intravenously dosing 200 mg/kg, and the tissues including heart, liver, spleen, lung and kidney, eyes, hippocampus, and prefrontal cortex were separated at different times. The concentrations of R-VGB and S-VGB in the plasma and tissues were measured using HPLC.

Results: Both S-VGB and R-VGB could be detected in the plasma of rats administered with VGB racemate, reaching Cmax at approximately 0.5 h with $t_{1/2}$ 2–3 h. There was no significant pharmacokinetic difference between the two enantiomers when VGB racemate was given 200 mg/kg and 100 mg/kg. However, when given at the dose of 50 mg/kg, S-VGB presented a shorter $t_{1/2}$ and a higher Cl/F than R-VGB, indicating a faster metabolism of S-VGB. Furthermore, when single enantiomer was administered respectively, S-VGB presented a slower metabolism than R-VGB, as indicated by a longer $t_{1/2}$ and MRT but a lower Cmax. Moreover, compared with the VGB racemate, the single enantiomers S-VGB and R-VGB had shorter $t_{1/2}$ and MRT, higher Cmax and AUC/D, and lower Vz/F and Cl/F, indicating the stronger oral absorption and faster metabolism of single enantiomer. In addition, regardless of VGB racemate administration or single enantiomer administration, S-VGB and R-VGB had similar characteristics in tissue distribution, and the content of S-VGB in hippocampus, prefrontal cortex and liver was much higher than that of R-VGB.

Conclusions: Although there is no transformation between S-VGB and R-VGB in vivo, those two enantiomers display certain disparities in the pharmacokinetics and tissue distribution, and interact with each other. These findings might be a possible interpretation for the pharmacological and toxic effects of VGB and a potential direction for the development and optimization of the single enantiomer S-VGB.

1. Introduction

Epilepsy is a common and serious brain disease, affecting about 65 million people worldwide(Maggiani and Bo, 2022). Aim to limit excitation and/or enhance inhibition(Elger and Schmidt, 2008), 17 s- and third-generation antiepileptic medications have been made available in clinical settings over the past three decades. However, besides the adverse effect of long-term medication, around one-third of epilepsy patients were reported to experience drug resistance even after getting the best treatment(Golyala and Kwan, 2017).

As we know, epilepsy is a paroxysmal and transient brain disorder caused by abnormal discharge of brain neurons(Rho and Boison, 2022;

Abbreviations: VGB, vigabatrin; S-VGB, S(+) enantiomer; R-VGB, R(-) enantiomer; GABA, γ-aminobutyric acid; GABA-T, γ-aminobutyric acid transaminase; pVFD, peripheral visual field deficits; HPLC, high performance liquid chromatography; IS, internal standard; $t_{1/2}$, elimination half-life; Tmax, peak time; Cmax, peak concentration; AUC/D, ratio of area under curve to dose; Vz/F, apparent volume of distribution; Cl/F, clearance; MRT, mean residence time.

Peer review under responsibility of King Saud University.

* Corresponding author at: School of Pharmacy, Anhui Medical University, 81 Mei-Shan Road, Hefei, Anhui 230032, PR China.
E-mail address: gejinfang@ahmu.edu.cn (J.-F. Ge).

https://doi.org/10.1016/j.jsps.2023.101934
Received 4 September 2023; Accepted 21 December 2023
Available online 23 December 2023

Thijs et al., 2019), and the imbalance of γ-aminobutyric acid (GABA) and glutamate has been demonstrated to play a crucial role(Sears and Hewett, 2021). GABA is the important inhibitory neurotransmitter, and glutamate is the metabolic precursor of GABA, which can be recycled through the tricarboxylic acid cycle to synthesize glutamate. It has long been demonstrated that direct or indirect interference with GABA-mediated neurotransmission could induce convulsive seizure activity in humans and experimental animals(Gale, 1992;Sousa et al., 2017), and seizure could be under control by the precisely tuned GABA delivery at the seizure onset(Slezia et al., 2019). (Sousa et al., 2017)(Ben-Menachem, 2011)(Ben-Menachem, 2011)(Sills and Rogawski, 2020)(Lux et al., 2005;O'Callaghan et al., 2017)(Yang et al., 2012)(Schwarz et al., 2016).

Vigabatrin (VGB), is a structural analogue of GABA. First synthesized in 1974 and developed as a potential anticonvulsant in the late 1970 s, VGB was approved in the United Kingdom then the U.S.A for the treatment of infantile spasms and refractory complex partial seizure epilepsy(French et al., 1996;Jung et al., 1977;Lortie et al., 1997). In China, the registration application for VGB pulvis was approved by the National Medical Products Administration in 2022. Based on its pharmacological activity of reducing the catabolism of GABA via irreversibly inhibiting GABA transaminase (GABA-T) (Sills and Rogawski, 2020), VGB can completely stop seizures in 75 % of cases of infantile spasm(Lux et al., 2005;O'Callaghan et al., 2017).(Sills and Rogawski, 2020) However, the clinical adverse effects, especially loss of visual field and abnormal brain imaging, have raised concerns about the safety of VGB, and greatly limit its widely application(Golec et al., 2021;Yang et al., 2012). It has been reported that VGB-treated patients are prone to peripheral visual field deficits(pVFD)(Ruether et al., 1998). Consistently, atrophy of the retinal fibrous layer has been observed in infants(Buncic et al., 2004) and adults(Wild et al., 2006) taking VGB, the mechanism of which has been partly ascribed to triggering retinal excitotoxicity via direct toxicity to retinal ganglion cells or secondary degeneration of photoreceptor cells(Vardi et al., 2000). Therefore, it is needed to optimize the structure or/and modify clinical scheme of VGB, enhancing the antiepileptic efficacy or/and reducing the retinal toxicity, especially the in-depth studies focusing on the pharmacokinetics, pharmacodynamics, and toxicology of VGB.

(Valdizán et al., 1999)(Rey et al., 1992)(Rey et al., 1990)(Elwes and Binnie, 1996)(Walters et al., 2019)Due to the warning form the discriminating pharmacological effect and adverse reaction of different isomers of chiral compounds such as thalidomide, a growing interest in enantiomerically pure substances has been spread in the field of pharmacology and medicinal chemistry. It has been identified that beyond the advantages of the drug administration as pure enantiomers, toxicity can be associated to the inactive enantiomer(Čižmáriková et al., 2020). Regarding the pharmacokinetics, the associated effects of a drug or its enantiomers in absorption, distribution, metabolism, excretion events, and toxicity are recognized(Lu, 2007). Stereoselectivity/enantioselectivity can be observed in all pharmacokinetic processes, important and well-known phenomena, mainly in the metabolism of xenobiotics (Mwamwitwa et al., 2020). Additionally, there is a more effective and lasting start of the desired effect, combined with a lower propensity to drug interactions, mediated in large part by the exploration of stereoselectivity not only in pharmacodynamics/pharmacokinetics but also in toxicity properties(Testa, 2015). However, despite the unequivocal advantages of the administration of pure enantiomers, many drugs are still commercialized as racemate(Mwamwitwa et al., 2020). VGB is clinically administered as a racemate, and data on its pharmacokinetics are scarce. Most of the published studies using rodents as experimental animals have been performed with non-continuous blood sampling, in which composite values were obtained from the execution of different individual animals at different time points following drug administration (Valdizán et al., 1999). Results from human studies showed that the Cl/F, $t_{1/2}$, and plasma exposure of the two enantiomers of VGB are varied (Rey et al., 1990), together with an unequally distribute profile in various tissues (Walters et al., 2019), although the absorption and metabolism of the two enantiomers are unaffected by one another(Elwes and Binnie, 1996). Moreover, it has been suggested that the antiepileptic mechanism of VGB should be ascribed to the S(+) enantiomer (S-VGB), but not R(-) enantiomer (R-VGB) (Sills and Rogawski, 2020). Therefore, it is rational to hypothesize that it is the stereoselectivity-associated difference of pharmacological and toxic effect that result in the clinical co-exit of the antiepileptic effect and adverse reactions for VGB racemate. To prove this hypothesis, it is necessary to systematically investigate the pharmacokinetic and tissue distribution characters of different enantiomers of VGB, compare with VGB racemate, and find a direction for structural optimization or clinical modification.

(Walters et al., 2021)The aim of the present study was to investigate the possible difference of the pharmacokinetics and tissue distribution among VGB racemate, single enantiomer R-VGB, and S-VGB, and to further explore the potential effects of R-VGB on S-VGB pharmacokinetics and the possibility of monotherapy with S-VGB. To fulfill this, VGB racemate, R-VGB, and S-VGB were parallelly given to rats by intragastric administration with gradient doses, and the blood samples were collected with a rational schedule. The concentrations of S-VGB and R-VGB in the plasma and tissues were measured, and the main parameters of pharmacokinetics and tissue distribution were analyzed and compared.

2. Materials and methods

2.1. Drugs and reagents

VGB, and its single enantiomer R-VGB and S-VGB, were obtained from Hefei Lifeon Pharmaceutical Co., Ltd (Hefei, China). Phthalaldehyde (OPA, HPLC grade), N-acetyl-L-cysteine (NAC, HPLC grade), methanol (HPLC grade), and acetonitrile (HPLC grade) were purchased from Sigma Aldrich Inc. USA. L-high arginine hydrochloride (internal standard, IS) and glacial acetic acid were purchased from Aladdin Reagent Co., Ltd. (Hefei, China), with analytical grade.

2.2. Animals

Adult male Sprague-Dawley rats, weighing 200–220 g, were purchased from Hefei Qinyuan Biotechnology Co.Ltd, China. They were housed by subgroup in contiguous cages under cyclic light (12-hour light/12-hour dark) with ad libitum access to water and a normal laboratory diet. An ambient temperature of around 25℃ was maintained and all rats were allowed to acclimatize to a new environment for about 1 week prior to experimentation. All animal care practices and experimental procedures were reviewed and approved by the Animal Experimentation Ethics Committee of Anhui Medical University in compliance with the National Institutes of Health Guide for the Care and Use of Laboratory Animals (NIH publication No. 85–23, revised 1985).

2.3. Sample treatment

Plasma: 100 μL plasma was taken and added with 100 μL pure water and 50 μL IS (0.04 mol/L), then 550 μL methanol precipitated protein was added, centrifuged at 2600 g at 4℃ for 20 min, 150 μL supernatant was taken, and 30 μL derivative was added into the sample for injection. The derivative was prepared by mixing 100 μL OPA (0.1 mol/L), 100 μL NAC (0.1 mol/L) and 800 μL sodium borate buffer salt solution (0.1 mol/L, pH = 10.2).

Tissue homogenates: Before detection, the tissue samples were weighed individually and homogenized in twice the volume of freshly prepared ice phosphate buffered brine pH 7.4. After centrifugation, 100 μL tissue homogenate was taken, which was then consistent with plasma treatment.

2.4. Chromatographic conditions

VGB concentrations in the plasma and tissue homogenates were measured by high performance liquid chromatography (HPLC) technique(Duhamel et al., 2017;Vermeij and Edelbroek, 1998) (Vermeij and Edelbroek, 1998)according to the reported method with a little modification. The HPLC system consisted of LC-20AT pumps, a DGU-20A5 degasser, a SIL-20AC autosampler and a SPD-20A UV–visible detector (Shimadzu, Kyoto, Japan). The separation was performed on a Supersil ODS2 -C18 column (3 mm, 150 mm*4.6 mm, Dalian Elite, China) with its specific pre-column. The temperature was set at 4 °C for the autosampler and 35 °C for the column compartment. The mobile phase was composed of two different solvents A and B, where A consisted in sodium acetate 55 mM in water, pH adjusted to 7.60 with 1 % acetic acid solution in water, and B consisted in 100 % acetonitrile. The flow rate was set at 1 mL/min and a gradient was used to separate correctly the two enantiomers of VGB. The following gradient elution program was used: an increase from 5 % to 17.5 % B within 25 min, to 35 % B from 25 to 26 min, and to 5 % B from 31 to 34 min. The analysis time was 40 min for each run. The UV wavelength detector was set at 340 nm and the sample size was 10 μL.

2.5. Validation of the analytical method

2.5.1. Specificity

Specificity was assessed by analyzing samples obtained from blank substrates and blank substrates with R-VGB, S-VGB, or IS added.

2.5.2. Absolute recovery

Absolute recovery is defined as the ratio of the analyte peak area of a standard sample to the that of a blank matrix with the same analyte concentration added.

2.5.3. Calibration curves

Calibration curves for plasma and tissue samples were established by linear regression of the peak area ratio of the different enantiomers of VGB to IS (x) against the nominal concentration of the different enantiomers of VGB (y). Calibration curves were constructed using nine R-VGB and S -VGB standards at concentrations ranging from 0.25 mg/L to 500 mg/L.

2.5.4. Precision and accuracy

The precision and accuracy of the method was evaluated by repeating the assay 5 times on the same day (intra-day) or different days (inter-day) for blank matrices added with different concentrations of R-VGB and S -VGB.

2.5.5. Stability experiments

Blood sample stabilities of S-VGB and R -VGB were assessed under two different conditions using five replicates of three standard concentrations. short-term stability was assessed by storage at room temperature for 4 h,and long-term stability was assessed by storage at − 20 °C for 2 weeks.

2.6. Pharmacokinetic study

In the pharmacokinetic experiment, rats were divided into 9 groups with 6 rats in each group: the rats received intragastric administration of VGB racemate, R-VGB, or S-VGB dosing 200 mg/kg, 100 mg/kg, or 50 mg/kg. Prior to blood sampling, the rats were fasted for one night and drank water freely. Blood samples were drawn from the angular vein, with volume of 300 μL at 0, 0.08, 0.25, 0.5, 1, 2, 3, 4, 6, 8, 10 and 12 h after intragastric administration of VGB, S-VGB, or R-VGB. In order to prevent the development of hypovolemia, an equivalent volume of heparinized saline was administered after each blood sampling. Blood samples were centrifuged at 4000 rpm for 10 min (4 °C),and plasma were stored frozen (−80 ± 5 °C) until analysis.

2.7. Tissue distribution study

In the tissue distribution experiment, the rats were divided into 3 groups with 6 rats in each group, intragastrically given VGB racemate, S-VGB, or R-VGB with the single dosage of 200 mg/kg. The rats were sacrificed 15 min, 1 h and 4 h after administration, respectively. Immediately, the heart, liver, spleen, lung, kidney, eye, hippocampus and prefrontal cortex were separated on ice and collected. After quickly frozen by liquid nitrogen, the samples were stored in − 80 ± 5 °C until analysis.

2.8. Statistical analysis of data

Calculation of pharmacokinetic parameters based on a one-compartment model with primary elimination using Phoenix WinNonlin8.3.5. The variables obtained were described by the means and standard deviation (SD). Data were compared using Student's t-test according to the size and condition of the groups formed. For this purpose, the IBM SPSS Statistics 23 and GraphPad Prism 8 were used. $P < 0.05$ was considered indicative of a statistically significant difference.

3. Result

3.1. Method validation

3.1.1. Specificity

Representative UV chromatograms of plasma, hippocampus and eye samples are shown in Fig. 1. IS, R-VGB and S-VGB were well separated with retention times of 16.3, 18.5 and 21.3 min, respectively, under the elution procedure above 40 min.

3.1.2. Absolute recovery

Absolute recoveries of R-VGB and S-VGB are shown in Table 1. Absolute recoveries of R-VGB and S-VGB in biological matrices were > 80 % (RSD ≤ 10 %) and all values were reproducible, ensuring accuracy.

3.1.3. Calibration curves

The calibration curves, correlation coefficients and linear ranges of R-VGB and S-VGB concentrations in the plasma and tissue homogenates are listed in Table 2. The calibration curves for all biologic matrices exhibited excellent linearity (R^2 > 0.999), ranging from 0.25 to 500 mg/L (ng/mg).

3.1.4. Precision and accuracy

As shown in Tables 3 and 4, the intra-day and inter-day precision of R-VGB and S-VGB in biological matrices were less than 3 %, and the results met the analytical requirements.

3.1.5. Stability experiments

Stabilities of R-VGB and S-VGB in rat plasma under different conditions are shown in Table 5. R-VGB and S-VGB are stable in plasma whether it was placed at room temperature for a short period or frozen for a long period (low standard concentration bias should be ± 20 %; medium and high standard concentration bias should be ± 15 %; the RSD should be ≤ 15 %).

3.2. Pharmacokinetic study of R-VGB and S-VGB in rats

3.2.1. Similar pharmacokinetic characteristics of S-VGB and R-VGB in rats administered with VGB racemate

According to Fig. 2a-2c, although given as the racemate form, distinct enantiomers of VGB were rapidly absorbed by rats following intragastric administration of various dosages. Plasma drug concentration was reached the Cmax within 0.5 ~ 1 h, and then decreasing

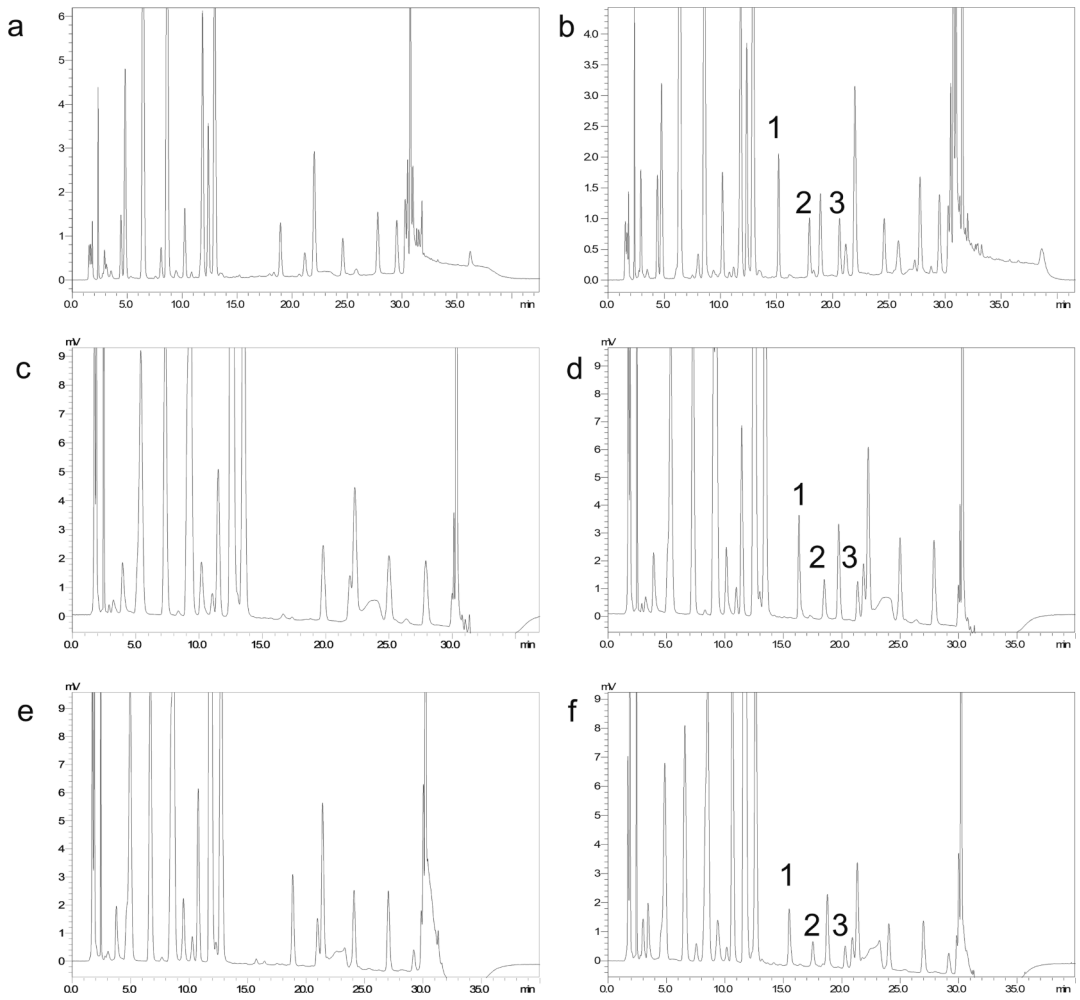

Fig. 1. Chromatograms of analytes recorded in HPLC from rat plasma, eye and hippocampal homogenates. a: blank plasma sample; b: blank plasma sample spiked with IS and VGB; c: blank eye sample; d: blank eye sample spiked with IS and VGB; e: blank hippocampus sample; f: blank hippocampus sample spiked with IS and VGB; VGB: Vigabatrin; 1:IS(L-high arginine hydrochloride); 2: R(-) enantiomer in VGB; 3: S(+) enantiomer in VGB.

Table 1
The extraction recovery of R-VGB and S-VGB in rat plasma and tissue homogenate (n = 5).

	Biologic matrices	1 mg/L		10 mg/L		100 mg/L	
		mean ± SD (%)	RSD (%)	mean ± SD (%)	RSD (%)	mean ± SD (%)	RSD (%)
R-VGB	Blood	94.51 ± 2.53	2.68	91.11 ± 0.52	0.57	91.42 ± 0.17	0.19
	Hippocampus	87.44 ± 3.02	3.46	91.39 ± 0.49	0.54	94.75 ± 1.67	1.76
	Prefrontal cortex	91.82 ± 4.11	4.48	91.76 ± 1.99	2.17	95.83 ± 0.79	0.82
	Eyes	88.23 ± 0.55	0.62	87.64 ± 0.81	0.93	95.49 ± 0.5	0.53
	Heart	88.15 ± 6.5	7.37	88.78 ± 1.35	1.52	96.58 ± 1.14	1.18
	Liver	91.49 ± 3.56	3.89	91 ± 1.38	1.52	92.86 ± 2.72	2.93
	Spleen	94.42 ± 4.4	4.66	90.57 ± 8.49	9.38	94.23 ± 1.6	1.7
	Lung	96.21 ± 6.79	7.06	98.32 ± 3.31	3.37	94.8 ± 3.45	3.64
	Kidney	100.66 ± 3.5	3.48	102.28 ± 2.5	2.44	99.78 ± 0.25	0.25
S-VGB	Blood	96.87 ± 4.02	4.15	85.68 ± 0.95	1.11	89.3 ± 0.06	0.07
	Hippocampus	92.02 ± 3.41	3.71	87.28 ± 1.09	1.24	91.87 ± 1.57	1.71
	Prefrontal cortex	93.56 ± 4.63	4.95	86.75 ± 0.53	0.61	90.87 ± 2.53	2.79
	Eyes	90.35 ± 1.67	1.85	86.04 ± 0.77	0.89	93.54 ± 0.57	0.61
	Heart	90.34 ± 4.63	5.12	84.78 ± 1.73	2.04	94.18 ± 1.32	1.4
	Liver	93.85 ± 3.23	3.44	87.83 ± 2.48	2.82	90.28 ± 2.35	2.61
	Spleen	97.47 ± 7.03	7.21	85.33 ± 7.83	9.18	89.67 ± 1.89	2.11
	Lung	96.49 ± 6.16	6.38	94.48 ± 2.14	2.27	93.57 ± 3.07	3.28
	Kidney	103.05 ± 3	2.92	100.4 ± 1.21	1.21	99.19 ± 0.61	0.61

exponentially. A one-compartment open model with first-order elimination was fitted to the plasma concentration–time profiles using nonlinear mixed effects modelling with first-order estimation. There was no other difference between the curves for the two enantiomers, except the fact that R-VGB had a little higher Cmax than S-VGB. The pharmacokinetic characteristics of R-VGB and S-VGB were further compared

Table 2
Calibration curves of R-VGB and S-VGB in rat biological samples.

	Biologic matrices	Calibration curves	Correlation coefficients (r^2)	Linear ranges (mg/ L)or(ng/mg)
R-VGB	Blood	y = 10.317x + 0.0427	0.9996	0.25–500
	Hippocampus	y = 11.296x − 0.0272	0.9999	0.25–500
	Prefrontal cortex	y = 12.577x − 0.0394	0.9997	0.25–500
	Eyes	y = 11.085x − 0.0603	0.9998	0.25–500
	Heart	y = 10.848x − 0.0263	0.9999	0.25–500
	Liver	y = 10.989x − 0.0221	0.9999	0.25–500
	Spleen	y = 10.85x + 0.1785	0.9998	0.25–500
	Lung	y = 10.986x − 0.2288	0.9998	0.25–500
	Kidney	y = 11.267x + 0.6866	0.9996	0.25–500
S-VGB	Blood	y = 10.282x + 0.0584	0.9994	0.25–500
	Hippocampus	y = 11.843x + 0.0216	0.9998	0.25–500
	Prefrontal cortex	y = 12.593x + 0.0221	0.9999	0.25–500
	Eyes	y = 11.029x + 0.0323	0.9996	0.25–500
	Heart	y = 10.582x + 0.016	0.9998	0.25–500
	Liver	y = 10.779x + 0.0539	0.9999	0.25–500
	Spleen	y = 10.574x + 0.4483	0.9997	0.25–500
	Lung	y = 10.780x − 0.1797	0.9998	0.25–500
	Kidney	y = 11.832x + 0.0938	0.9998	0.25–500

Table 3
Intra-day precision of R-VGB and S-VGB in rat plasma and tissue homogenates (n = 5).

	Biologic matrices	1 mg/L		10 mg/L		100 mg/L	
		Mean ± SD	RSD (%)	Mean ± SD	RSD (%)	Mean ± SD	RSD (%)
R-VGB	Blood	1.026 ± 0.025	2.50 %	9.839 ± 0.096	1.00 %	98.055 ± 0.47	0.50 %
	Hippocampus	1.006 ± 0.02	2.00 %	10.166 ± 0.139	1.40 %	100.332 ± 1.714	1.70 %
	Prefrontal cortex	0.994 ± 0.019	1.90 %	10.092 ± 0.015	0.10 %	100.532 ± 0.548	0.50 %
	Eyes	1 ± 0.018	1.80 %	9.863 ± 0.06	0.60 %	97.712 ± 0.268	0.30 %
	Heart	1.008 ± 0.01	1.00 %	9.994 ± 0.213	2.10 %	100.603 ± 1.617	1.60 %
	Liver	0.992 ± 0.008	0.80 %	9.906 ± 0.113	1.10 %	97.629 ± 0.507	0.50 %
	Spleen	1.007 ± 0.019	1.90 %	9.962 ± 0.182	1.80 %	98.949 ± 0.593	0.60 %
	Lung	1.008 ± 0.014	1.40 %	10.22 ± 0.05	0.50 %	101.26 ± 1.119	1.10 %
	Kidney	0.997 ± 0.015	1.50 %	10.085 ± 0.15	1.50 %	100.349 ± 1.942	1.90 %
S-VGB	Blood	1.028 ± 0.039	3.80 %	9.693 ± 0.078	0.80 %	100.361 ± 0.561	0.60 %
	Hippocampus	1.009 ± 0.018	1.80 %	10.26 ± 0.059	0.60 %	101.807 ± 0.745	0.70 %
	Prefrontal cortex	1.006 ± 0.021	2.10 %	10.057 ± 0.143	1.40 %	102.536 ± 0.331	0.30 %
	Eyes	1.006 ± 0.012	1.20 %	9.973 ± 0.185	1.90 %	100.414 ± 0.442	0.40 %
	Heart	0.998 ± 0.02	2.00 %	10.036 ± 0.112	1.10 %	101.907 ± 1.22	1.20 %
	Liver	1.013 ± 0.014	1.40 %	9.997 ± 0.044	0.40 %	102.789 ± 0.423	0.40 %
	Spleen	1.005 ± 0.02	2.00 %	10.103 ± 0.024	0.20 %	102.527 ± 0.691	0.70 %
	Lung	1.005 ± 0.007	0.70 %	10.098 ± 0.172	1.70 %	100.615 ± 1.236	1.20 %
	Kidney	1.017 ± 0.007	0.70 %	10.135 ± 0.261	2.60 %	102.275 ± 1.449	1.40 %

Table 4
Inter-day precisions of R-VGB and S-VGB in rat plasma and tissue homogenates (n = 5).

	Biologic matrices	1 mg/L		10 mg/L		100 mg/L	
		Mean ± SD	RSD (%)	Mean ± SD	RSD (%)	Mean ± SD	RSD (%)
R-VGB	Blood	1.004 ± 0.038	3.80 %	10.106 ± 0.216	2.10 %	100.8 ± 2.007	2.00 %
	Hippocampus	1.009 ± 0.007	0.70 %	9.918 ± 0.118	1.20 %	98.851 ± 0.919	0.90 %
	Prefrontal cortex	0.997 ± 0.02	2.10 %	9.895 ± 0.141	1.40 %	99.226 ± 0.959	1.00 %
	Eyes	1.001 ± 0.019	1.90 %	9.976 ± 0.167	1.70 %	97.491 ± 0.327	0.30 %
	Heart	1.01 ± 0.014	1.40 %	9.874 ± 0.122	1.20 %	98.095 ± 0.726	0.70 %
	Liver	1.001 ± 0.017	1.70 %	9.935 ± 0.158	1.60 %	100.727 ± 1.315	1.30 %
	Spleen	0.99 ± 0.017	1.70 %	10.065 ± 0.153	1.50 %	100.428 ± 1.708	1.70 %
	Lung	1.003 ± 0.011	1.10 %	9.938 ± 0.169	1.70 %	100.204 ± 1.853	1.80 %
	Kidney	1.012 ± 0.02	2.00 %	9.911 ± 0.113	1.10 %	98.209 ± 0.348	0.40 %
S-VGB	Blood	1.03 ± 0.008	0.80 %	10.109 ± 0.229	2.30 %	102.413 ± 1.517	1.50 %
	Hippocampus	1.009 ± 0.014	1.30 %	10.132 ± 0.175	1.70 %	101.473 ± 1.02	1.00 %
	Prefrontal cortex	1.006 ± 0.021	2.10 %	9.992 ± 0.103	1.00 %	100.714 ± 1.342	1.30 %
	Eyes	0.997 ± 0.021	2.10 %	9.884 ± 0.126	1.30 %	100.162 ± 1.799	1.80 %
	Heart	1.009 ± 0.007	0.70 %	9.949 ± 0.207	2.10 %	99.863 ± 1.83	1.80 %
	Liver	1.015 ± 0.028	2.80 %	10.076 ± 0.116	1.10 %	100.521 ± 2.218	2.20 %
	Spleen	1 ± 0.018	1.80 %	10.204 ± 0.137	1.30 %	101.607 ± 1.951	1.90 %
	Lung	1.012 ± 0.016	1.60 %	10.188 ± 0.2	2.00 %	102.279 ± 1.435	1.40 %
	Kidney	1.013 ± 0.016	1.60 %	10.078 ± 0.032	0.30 %	102.07 ± 1.245	1.20 %

Table 5
The stability of R-VGB and S-VGB in rat plasma (n = 5).

Storage condition	dose	R-VGB		S-VGB	
		Mean ± SD	RSD (%)	Mean ± SD	RSD (%)
Kept at room temperature for 2 h	2.5 mg/L	2.628 ± 0.035	1.31 %	2.564 ± 0.058	2.25 %
	12.5 mg/L	12.383 ± 0.132	1.07 %	12.494 ± 0.188	1.50 %
	50 mg/L	50.195 ± 0.51	1.02 %	51.284 ± 0.672	1.31 %
Kept at − 20 °C for 2 weeks	2.5 mg/L	2.604 ± 0.115	4.43 %	2.604 ± 0.057	2.19 %
	12.5 mg/L	12.578 ± 0.267	2.12 %	12.595 ± 0.172	1.37 %
	50 mg/L	49.113 ± 2.215	4.51 %	50.409 ± 1.916	3.80 %

and shown in Table 6. There was no significant pharmacokinetic difference between the two enantiomers when VGB racemate was given dosing 200 mg/kg and 100 mg/kg. However, when given at the dose of 50 mg/kg, S-VGB presented a shorter $t_{1/2}$(t = 3.327,P = 0.005) and a higher Cl/F(t = 2.261,P = 0.048) than R-VGB, indicating a faster metabolism of S-VGB.

3.2.2. S-VGB has a longer metabolic time and a slower absorption rate in rats than R-VGB in rats when given single enantiomers, respectively

After administration of a single enantiomer, the drug concentration–time curve was depicted in Fig. 2d-2f, which showed overall consistency with that of VGB racemate, and there was no transformation between S-VGB and R-VGB in vivo. However, the maximum peak concentration of S-VGB was significantly lower than that of R-VGB, with a relatively slow downward trend. As shown in Table 7, there was a significant difference between the pharmacokinetic parameters of the two enantiomers. In comparison to R-VGB, the $t_{1/2}$ (t = 2.284,P = 0.047) and MRT (t = 3.772,P = 0.002) of S-VGB was significantly longer, and the Cmax(t = 5.004,P = 0.001) was lower at high doses. In addition, S-VGB had a slightly higher Vz/F and a slightly longer Tmax, with similar trends across doses.

3.2.3. S-VGB and R-VGB affect each other's pharmacokinetics in rats

Additionally, we analyzed the pharmacokinetic interactions between R-VGB and S-VGB by comparing the pharmacokinetic parameters among groups administrated with VGB as a single enantiomer or racemate. As demonstrated in Table 8, when given as the single enantiomer, S-VGB exhibited significantly shorter $t_{1/2}$ (t = 2.176,P = 0.047) and MRT(t = 4.164,P = 0.002), markedly higher Cmax (t = 7.140,P = 0.000), increased AUC/D (t = 8.354,P = 0.000), decreased Vz/F (t = 4.739,P = 0.000), and reduced Cl/F (t = 6.120,P = 0.000), compared to racemate administration. Similar findings were found for R-VGB. These results suggest a potential interaction between R-GVB and S-VGB when given as a racemate, resulting in the prolonged their $t_{1/2}$, slowed metabolism, and extended tissue distribution, together with a decreased bioavailability of the corresponding other one.

3.3. Dynamic tissue distribution of S-VGB and R-VGB in rats

3.3.1. Higher accumulation of S-VGB than R-VGB in eye, hippocampus, prefrontal cortex, and liver in rats administered with VGB racemate

The dynamic tissues distribution is shown in Fig. 3, S-VGB was slightly higher than R-VGB (t = 3.020,P = 0.027) in the eyes at 4 h after administration of VGB racemate (Fig. 3a). As shown in Fig. 3b and 3c, S-VGB exhibited significantly higher abundance in the hippocampus (t = 7.655, P = 0.000) and prefrontal cortex (t = 3.458, P = 0.000) compared to R-VGB at all time points. The distribution of VGB in the heart, liver, spleen, lung, and kidney of rats is shown in Fig. 3d-3f, with the highest content of the two enantiomers in the kidney, followed by the liver. Furthermore, S-VGB was substantially more abundant in the liver than R-VGB at 15 min (t = 5.587, P = 0.000) and 1 h (t = 3.417, P = 0.008).

3.3.2. Higher accumulation of S-VGB than R-VGB in eye, hippocampus, prefrontal cortex and liver in rats administered individually with a single enantiomer

The two single enantiomers were administered to rats individually and their tissue distribution profiles were shown in Fig. 4. Consistent with the results of given with VGB racemate, the intraocular content of S-VGB was slightly higher than that of R-VGB all the time, with a significant difference at 1 h (t = 2.985,P = 0.029) . The concentration of S-VGB in the prefrontal cortex (t = 6.181, P = 0.002) and the liver was

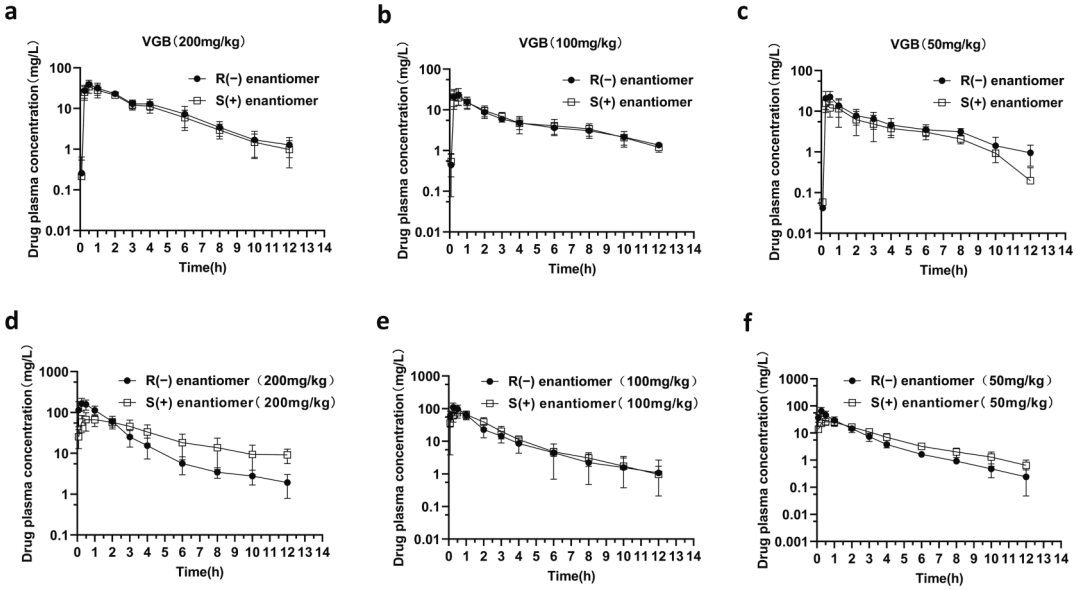

Fig. 2. Plasma concentration–time curves after the intragastric administration of VGB racemate ang its single enantiomers a: VGB racemate (200 mg/kg) was gavaged in rats; b: VGB racemate (100 mg/kg) was gavaged in rats; c: VGB racemate (50 mg/kg) was gavaged in rats; d: single enantiomer R-VGB(200 mg/kg) and S-VGB(200 mg/kg) were gavaged separately in rats; e: single enantiomer R-VGB(100 mg/kg) and S-VGB(100 mg/kg) were gavaged separately in rats; f: single enantiomer R-VGB(50 mg/kg) and S-VGB(50 mg/kg) were gavaged separately in rats. Data are expressed as mean ± SD, n = 6.

Table 6
Pharmacokinetic parameters of R-VGB and S-VGB after gavage of different doses of VGB racemate in rats (Mean ± SD, n = 6).

Dose(mg/kg)	Pharmacokinetic parameters	VGB racemate	
		R-VGB	S-VGB
200	$t_{1/2}$ (h)	2.285 ± 0.556	2.269 ± 0.450
	Tmax(h)	0.406 ± 0.129	0.719 ± 0.558
	Cmax(mg/L)	40.362 ± 9.947	34.421 ± 10.589
	AUC/D(h*kg*mg/L/mg)	1.341 ± 0.183	1.199 ± 0.192
	Vz/F (L/kg)	2.444 ± 0.505	2.727 ± 0.492
	Cl/F(L/h/kg)	0.751 ± 0.098	0.847 ± 0.145
	MRT(h)	3.575 ± 0.910	3.612 ± 0.840
100	$t_{1/2}$ (h)	3.035 ± 0.730	2.836 ± 0.542
	Tmax(h)	0.468 ± 0.088	0.406 ± 0.129
	Cmax(mg/L)	27.566 ± 13.513	25.121 ± 12.211
	AUC/D(h*kg*mg/L/mg)	1.576 ± 0.161	1.603 ± 0.260
	Vz/F (L/kg)	2.775 ± 0.811	2.594 ± 0.881
	Cl/F(L/h/kg)	0.630 ± 0.072	0.624 ± 0.108
	MRT(h)	4.692 ± 1.634	4.851 ± 1.421
50	$t_{1/2}$ (h)	2.705 ± 0.473	1.940 ± 0.446**
	Tmax(h)	0.500 ± 0.327	0.437 ± 0.347
	Cmax(mg/L)	21.033 ± 6.624	18.632 ± 8.624
	AUC/D(h*kg*mg/L/mg)	2.564 ± 0.833	1.904 ± 0.469
	Vz/F (L/kg)	1.599 ± 0.378	1.493 ± 0.297
	Cl/F(L/h/kg)	0.422 ± 0.118	0.548 ± 0.144*
	MRT(h)	4.336 ± 0.707	3.695 ± 0.845

$t_{1/2}$: elimination half-life; Tmax: peak time; Cmax: peak concentration; AUC/D: ratio of area under curve to dose; Vz/F: apparent volume of distribution; Cl/F: clearance; MRT: mean residence time.
* $P < 0.05$.
** $P < 0.01$compared with R-VGB.

Table 7
Pharmacokinetic parameters of R-VGB and S-VGB after respectively gavage of different doses of single enantiomer R-VGB and S-VGB (Mean ± SD, n = 6).

Dose(mg/kg)	Pharmacokinetic parameters	Single enantiomer	
		R-VGB	S-VGB
200	$t_{1/2}$ (h)	2.063 ± 0.405	2.909 ± 0.966*
	Tmax(h)	0.438 ± 0.259	0.906 ± 0.706
	Cmax(mg/L)	174.818 ± 46.893	83.254 ± 20.780**
	AUC/D(h*kg*mg/L/mg)	1.745 ± 0.48	2.185 ± 0.519
	Vz/F (L/kg)	1.735 ± 0.284	1.922 ± 0.649
	Cl/F(L/h/kg)	0.604 ± 0.156	0.472 ± 0.143
	MRT(h)	2.093 ± 0.769	4.923 ± 1.658**
100	$t_{1/2}$ (h)	1.799 ± 0.423	2.301 ± 0.59
	Tmax(h)	0.344 ± 0.129	0.76 ± 0.584
	Cmax(mg/L)	125.499 ± 52.341	86.382 ± 17.652
	AUC/D(h*kg*mg/L/mg)	1.981 ± 0.676	1.907 ± 0.144
	Vz/F (L/kg)	1.427 ± 0.589	1.701 ± 0.364
	Cl/F(L/h/kg)	0.553 ± 0.184	0.518 ± 0.045
	MRT(h)	1.838 ± 0.379	2.211 ± 0.448
50	$t_{1/2}$ (h)	1.796 ± 0.221	2.268 ± 0.500*
	Tmax(h)	0.270 ± 0.160	0.594 ± 0.265**
	Cmax(mg/L)	67.880 ± 22.749	29.098 ± 6.716**
	AUC/D(h*kg*mg/L/mg)	1.706 ± 0.386	1.732 ± 0.276
	Vz/F (L/kg)	1.466 ± 0.560	1.853 ± 0.373
	Cl/F(L/h/kg)	0.544 ± 0.173	0.576 ± 0.091
	MRT(h)	1.703 ± 0.353	2.712 ± 0.399**

$t_{1/2}$: elimination half-life; Tmax: peak time; Cmax: peak concentration; AUC/D: ratio of area under curve to dose; Vz/F: apparent volume of distribution; Cl/F: clearance; MRT: mean residence time.
* $P < 0.05$.
** $P < 0.01$ compared with R-VGB.

persistently also significantly higher than that of R-VGB (Fig. 4c and 4e). Additionally, the two single enantiomers were predominantly distributed in the kidney, followed by the liver. Moreover, the characteristics of S-VGB preferential aggregation were also shown in hippocampus, heart, spleen, lungs, and kidneys, with no significant difference.

4. Discussion

In the present study, we investigated the characteristics of the pharmacokinetic and tissue distribution of VGB and its two enantiomers, S-VGB and R-VGB by HPLC. The results demonstrated that HPLC could be an effective and reliable technique for the separation and detection of S-VGB and R-VGB, with satisfactory specificity, extraction recovery, and precision. Moreover, our results showed that both S-VGB and R-VGB were detectable in the plasma and tissues of rats administered with VGB racemate, showing similar but a bit different pharmacokinetic property. The absorption rates of R-VGB and S-VGB were notably rapid, whether administered in racemate or enantiomer form. They reached Cmax at approximately 0.5 h and then exhibited a rapid exponential decline following a first-order rate. When VGB was administered as a racemate, S-VGB had a shorter $t_{1/2}$ and higher Cl/F only at the dose of 50 mg/kg, but not 200 mg/kg and 100 mg/kg. However, when given individually as the form of a single enantiomer, respectively, S-VGB had a longer $t_{1/2}$ and MRT, accompanied with a lower Cmax. In addition, compared to racemate administration, S-VGB and R -VGB exhibited significantly shorter $t_{1/2}$ and MRT, markedly higher Cmax, increased AUC/D, decreased Vz/F, and reduced Cl/F. Moreover, the tissue distribution profile of S-VGB was consistent in the two administration form, and R-VGB the same was similar. Furthermore, the content of S-VGB in the hippocampus, prefrontal cortex and liver was much higher than that of R-VGB. These results demonstrated that S-VGB had a longer retention time and wider distribution in rats compared to R-VGB. Moreover, our results indicated that when given as racemate form, the two enantiomers of VGB racemate may interact with each other, influence the metabolism and distribution, and ultimately lead to the discriminating pharmacological and toxic effect with potential stereoselectivity.

A reliable detection is the basis for investigations focusing on pharmacokinetics and tissue distribution. The available assays for detecting VGB enantiomers in biological matrices include HPLC, LC-MS and GC–MS(Al-Majed, 2009;Duhamel et al., 2017;Hložek et al., 2016). However, these methods require a pre-column derivatization step in order to add a chromophore to the enantiomers to improve sensitivity, and/or to produce diastereoisomers which can be easily separated. The derivative reaction of OPA-NAC was chosen in combination with conventional HPLC because of the rapid reaction at room temperature without any stopping procedure(Vermeij and Edelbroek, 1998). In the present study, we successfully isolated and detected the plasma and tissue concentration of R-VGB and S -VGB by HPLC, and results showed that the method was accurate and reliable, as indicated by the satisfactory parameters of methodological validation including specificity, absolute recovery, calibration curves, and intra-day and inter-day precision.

The $t_{1/2}$ and Cl/F values reflect the rate at which drugs are eliminated from the body and are closely related to the safety and efficacy of medications. These parameters also serve as important considerations for drug prescription, as they help determine appropriate dosing regimens and intervals to maintain therapeutic drug levels and minimize the risk of accumulation or subtherapeutic concentrations(Kowalski, 1994). Animal studies had shown that in rats injected intraperitoneally, the $t_{1/2}$ and Cmax of VGB was about 1.5 h and 0.4 h, respectively(Tong et al., 2007). Inconsistently, results of clinical investigations showed that the $t_{1/2}$ and Cmax of both S-VGB and R-VGB was 6–8 h and 1–2 h in adult males, and the Cl/F was 0.1 L/h/kg (Haegele and Schechter, 1986). However, the $t_{1/2}$ of S-VGB was reported to be approximately 6.5 h, which was significantly longer than that of R-VGB(approximately 2.5 h) in children (Nagarajan et al., 1993). In the present study, when VGB was

Table 8
Differences in pharmacokinetic parameters between the single enantiomer and the VGB racemate (Mean ± SD, n = 6).

	Pharmacokinetic parameters	R-VGB in VGB	single enantiomer R-VGB	S-VGB in VGB	single enantiomer S-VGB
VGB racemate (200 mg/kg) vs. single enantiomer (100 mg/kg)	$t_{1/2}$(h)	2.285 ± 0.556	1.799 ± 0.423	2.269 ± 0.450	2.301 ± 0.59
	Tmax(h)	0.406 ± 0.129	0.344 ± 0.129	0.719 ± 0.558	0.76 ± 0.584
	Cmax(mg/L)	40.362 ± 9.947	125.499 ± 52.341**	34.421 ± 10.589	86.382 ± 17.652##
	AUC/D (h*kg*mg/L/mg)	1.341 ± 0.183	1.981 ± 0.676**	1.199 ± 0.192	1.907 ± 0.144##
	Vz/F (L/kg)	2.444 ± 0.505	1.427 ± 0.589**	2.727 ± 0.492	1.701 ± 0.364##
	Cl/F(L/h/kg)	0.751 ± 0.098	0.553 ± 0.184*	0.847 ± 0.145	0.518 ± 0.045##
	MRT(h)	3.575 ± 0.910	1.838 ± 0.379**	3.612 ± 0.840	2.211 ± 0.448##
VGB racemate (100 mg/kg) vs. single enantiomer (50 mg/kg)	$t_{1/2}$(h)	3.035 ± 0.730	1.796 ± 0.221**	2.836 ± 0.542	2.268 ± 0.5#
	Tmax(h)	0.468 ± 0.088	0.270 ± 0.160**	0.406 ± 0.129	0.594 ± 0.265
	Cmax(mg/L)	27.566 ± 13.513	67.880 ± 22.749**	25.121 ± 12.211	29.098 ± 6.716
	AUC/D (h*kg*mg/L/mg)	1.576 ± 0.161	1.706 ± 0.386	1.603 ± 0.260	1.732 ± 0.276
	Vz/F (L/kg)	2.775 ± 0.811	1.466 ± 0.560**	2.594 ± 0.881	1.853 ± 0.373##
	Cl/F(L/h/kg)	0.630 ± 0.072	0.544 ± 0.173	0.624 ± 0.108	0.576 ± 0.091
	MRT(h)	4.692 ± 1.634	1.703 ± 0.353**	4.851 ± 1.421	2.712 ± 0.399##

$t_{1/2}$: elimination half-life; Tmax: peak time; Cmax: peak concentration; AUC/D: ratio of area under curve to dose; Vz/F: apparent volume of distribution; Cl/F: clearance; MRT: mean residence time.
* P < 0.05.
** P < 0.01 compared with R-VGB in VGB.
# P < 0.05.
P < 0.01 compared with S-VGB in VGB.

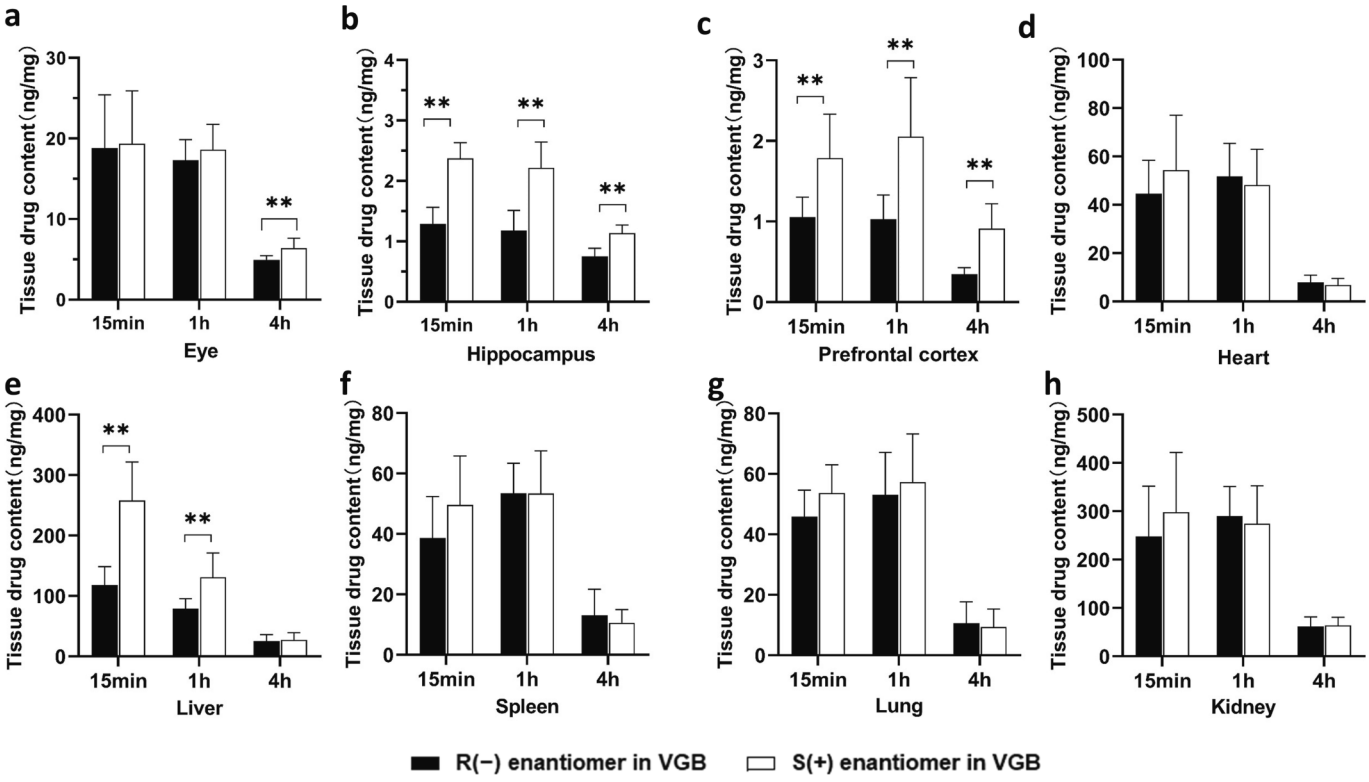

Fig. 3. Dynamic distribution of VGB racemate (200 mg/kg) in different tissues in rats a-h indicate the differences in the contents of S-VGB and R-VGB in the eye, hippocampus, prefrontal cortex, heart, liver, spleen, lungs and kidneys, respectively, at different times after VGB racemate (200 mg/kg) gavage in rats. Data are expressed as mean ± SD, n = 6. *P < 0.05, **P < 0.01 compared with R-VGB.

administered as a racemate, S-VGB and R-VGB had similar pharmacokinetic profiles at doses of 200 mg/kg and 100 mg/kg. The $t_{1/2}$ of R-VGB and S-VGB was about 2–3 h, the Cl/F was 0.4–0.8 L/h/kg, and the blood concentration reached a maximum at around 0.5 h. However, at dose of 50 mg/kg, S-VGB had a shorter $t_{1/2}$ and a higher Cl/F than R-VGB, suggesting a quicker elimination rate of S-VGB. It was worth noting that these values were in line with the findings in animal study(Tong et al., 2007), but the $t_{1/2}$ and CL/F were considerably shorter than that observed in the human body(Nagarajan et al., 1993). The discrepancy could be ascribed to species difference in drug metabolism and clearance mechanisms. These results indicated that there may be differences in the pharmacokinetic profiles of R-VGB and S-VGB in the racemate.

To further investigated the potential pharmacokinetic difference between R-VGB and S-VGB. We compared the pharmacokinetic parameters of S-VGB and R-VGB in rats administered with a single enantiomer. (Wang et al., 2019)(Nagarajan et al., 1993)(Haegele and

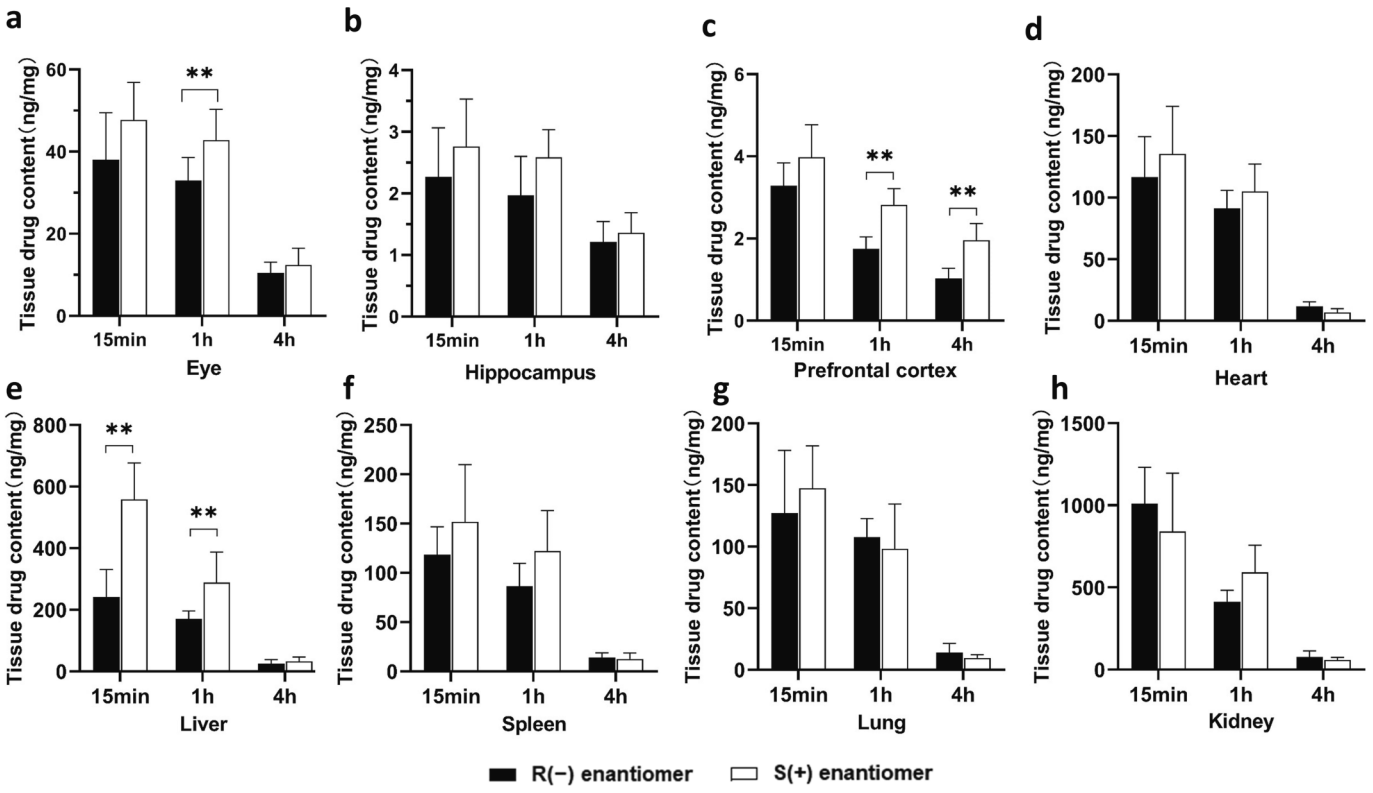

Fig. 4. Dynamic distribution of single enantiomer R-VGB (200 mg/kg) and S-VGB (200 mg kg) in different tissues in rats a-h indicate the differences in the contents of S-VGB and R-VGB in the eye, hippocampus, prefrontal cortex, heart, liver, spleen, lungs and kidneys, respectively, at different times after single enantiomer R-VGB (200 mg/kg) and S-VGB (200 mg kg) gavage in rats. Data are expressed as mean ± SD, n = 6. *P < 0.05, **P < 0.01 compared with R-VGB.

Schechter, 1986)(Tong et al., 2007)The results showed that S-VGB has a slightly longer $t_{1/2}$ and MRT than R-VGB. MRT is defined as the time at which up to 63.2 % of the drug is eliminated in vivo, but it can only be calculated when the drug exhibits linear drug dynamics. However, there was no significant difference in Cl/F, which could probably be interpreted by the strong reabsorption capacity in the renal tubules for VGB (Patsalos, 2013)(Scotcher et al., 2016). In addition, S-VGB had a lower Cmax and longer Tmax than that of R-VGB. Tmax, Cmax and AUC/D reflect the speed of drug absorption into the blood, an important indicator for evaluating the degree of drug absorption, and indirectly reflecting the size of the bioavailability of the drug. In line with this, it was reported that the Cmax of S-VGB was lower than that of R-VGB, with a ratio of approximately 1:2, and the urine recovery rate (49 %) was also lower than that of R-VGB (65 %) in humans(Haegele and Schechter, 1986). While Vz/F of S -VGB was slightly larger than R-VGB. Vz/F refers to the total volume of body fluid when the drug concentration in the whole body is the same as the blood under conditions in which the drug is completely distributed and its concentrations in all organs reach equilibrium. The higher the value of Vz/F, the more concentrated the medication could be dispersed in an organ or a variety of tissues (Wang et al., 2019). (Haegele and Schechter, 1986)According to this, S-VGB entered tissues more readily than R-VGB and/or irreversibly bound to GABA-T(Ben-Menachem, 2011), which might account for its reduced plasma exposure and urine recovery rate. These results indicated significant differences in the pharmacokinetic profiles of S-VGB and R-VGB, with slower absorption and longer metabolic time of S-VGB compared to R-VGB. Due to our finding and clinical results, the pharmacokinetics of R-VGB and S-VGB were inconsistent, especially the difference of pharmacokinetic characteristics of R-VGB in children and adults(Haegele and Schechter, 1986;Nagarajan et al., 1993). Therefore, we concluded that R-VGB might be a destabilizing factor in the efficacy and toxicity of VGB racemate in the treatment of epilepsy.

Based on the inconsistent results of pharmacokinetic differences between R-VGB and S-VGB after racemate administration or single enantiomer administration, we hypothesized that there might be mutual interference between the two in the pharmacokinetics. By analyzing the pharmacokinetic parameters of the VGB racemate and the single enantiomer, the $t_{1/2}$, MRT and Vz/F of R-VGB and S-VGB after administration of single enantiomer were significantly smaller than that of the racemate, the Cmax and AUC/D were significantly increased. These results suggested that the presence of R-VGB decreases the absorption of S-VGB and prolongs the metabolism time of S-VGB, which might affect the failure of S-VGB to reach the effective concentration of anti-epilepsy in a short period of time, and the long metabolic time would cause the accumulation in tissues and organs, which might in turn increase the retinal damage and potential systemic side effects. Consistently, results of our ongoing work (unpublished data) suggested a higher antiepileptic effect, higher LD50, but lower retinal toxicity of S-VGB than VGB racemate and R-VGB. Therefore, it is possible that the single enantiomer S-VGB has a superior drug-forming potential over the VGB racemate, with its faster absorption and higher bioavailability to rapidly reach the lesion to produce antiepileptic effects, and its shorter metabolism time reduces the possibility of cumulative toxicity and precludes interference of R-VGB with S-VGB and its potential toxicity. Although Vz/F was relatively small, single enantiomer S-VGB also showed excellent tissue immersion ability in tissue distribution experiments.

Studies on both humans and animals have revealed that the prefrontal cortex and hippocampus are epileptogenic regions that are crucial in the development of temporal lobe seizures (Bonini et al., 2014; Huberfeld et al., 2015;Lado et al., 2002;Li et al., 2021). VGB has been extensively studied to investigate its effects on the morphological, synaptic, and functional changes in the hippocampus and retina during seizures associated with epilepsy. VGB can lessen the hippocampus's epilepsy-induced neuronal damage(Kang et al., 2003) and cause retinal impairment linked to variations in electroretinogram readings (Ruether et al., 1998). Present study showed that, the concentration of S-VGB is

higher than R-VGB in the eye, hippocampus, prefrontal cortex and liver, regardless of racemate or single enantiomer. In line with this, it was reported that S-VGB preferentially aggregates in retinal and brain tissues of mouse compared to R-VGB, with a ratio of 6:1 and 2:1 (Walters et al., 2019).X. Tong et al. investigated the pharmacokinetics of VGB in cerebrospinal fluid and demonstrated that the rate of elimination of VGB in cerebrospinal fluid was significantly lower than that in blood(Tong et al., 2007). Consistently, studies have shown that the increase in GABA concentration in the central nervous system of mice treated with a single dose of VGB persisted much long, revealing that the biologic half-life of the drug is measured in days, not hours(Ben-Menachem, 2011). These results suggest that the relatively fast rate of metabolism of the single enantiomer S-VGB in the blood might not affect the duration of its effects in the brain. (Tong et al., 2007)(Walters et al., 2019)(Tong et al., 2007) However, the preferential aggregation of S-VGB in the eye has irreversible damage to the retina. Studies had shown that S-VGB preferentially accumulates in the retina compared to R-VGB, and only S-VGB acts on GABA-T, causing an increase in intraocular GABA concentration. This, in turn, causes taurine transporter to bind competitively, leading to taurine deficiency in the retina (Walters et al., 2021), which damages cone and reticular cells (Jammoul et al., 2010). These results indicated that single enantiomer and racemate have similar tissue distribution trends, and single enantiomer S-VGB still retained the ability to penetrate rapidly into brain tissue. Although single enantiomer S-VGB could not avoid potential retinal toxicity, its rapid metabolism rate compared to racemates and the absence of the potential effects of R-VGB might have reduced overall toxicity to some extent in patients with epilepsy.

The potential adverse effects of VGB on the heart, liver, spleen, lung, and kidney have not been extensively studied. However, approximately 80 % of the administered dose is excreted through the kidneys in its original form(Patsalos, 2013). In this experiment, VGB exhibited the highest distribution in the kidney, followed by the liver, and S-VGB was much more abundant in the liver than R-VGB. Anticonvulsants were blamed for 40 of the 899 drug-related liver injuries that were included in a prospective analysis from 2004 to 2013, however none were related to VGB(Chalasani et al., 2015). Research on animals revealed that VGB had no discernible impact on the cytochrome P450 enzyme activity in rats, dogs, or monkeys, and that there was no liver metabolic change (Durham et al., 1993;Elwes and Binnie, 1996;Gibson et al., 1990). Nevertheless, after taking VGB for 10 months, some female patients with episodic diseases experienced acute hepatitis, mostly with liver cell destruction, according to reports in the literature(Locher et al., 2001), and there are were studies that the liver damage caused by VGB may be caused by allergies (Vigabatrin, 2012). In individuals with severe renal failure, case reports had demonstrated that VGB has a terminal elimination $t_{1/2}$ of up to 41 h (Bachmann et al., 1996). Therefore, further studies about the specific effects of VGB on the liver and kidney are required.

This study has several deficiencies that should be improved in our further studies. Firstly, the relatively small sample size limits the significance of the present results. Second, although this experiment avoided the bias caused by discontinuous blood collection and was supplemented with an equal volume of heparinized saline after each blood collection, the effects of stress and loss of body fluids could not be ruled out with continuous blood collection. Moreover, the pharmacokinetics of VGB ultimately give the basis for clinical dosing regimens, but there are species-specific differences between humans and rodents that we cannot avoid at the moment. Finally, although the pharmacokinetic profile of the single enantiomer differs from that of the VGB racemate, the detailed mechanism was not explored in the present study.

5. Conclusion

In summary, R-VGB and S-VGB exhibit distinct pharmacokinetics and tissue distribution, and they also affect each other's in vivo absorption, distribution, and metabolism, even without mutual conversion between the two enantiomers. Based on the recognition of the interference of the inactive enantiomer R-VGB with the pharmacokinetics of S-VGB and its potential toxicity, the active enantiomer S-VGB possesses more advantages of the VGB racemate, such as purer antiepileptic efficacy and the exclusion of the interference of the inactive enantiomer, which provides novel information on dosing strategies or contributes to the study of the single enantiomer S-VGB as a separate drug. Therefore, pharmacological and toxicological studies of the single enantiomer S-VGB are essential in the future to facilitate its wider clinical application.

Declaration of competing interest

The authors declare that they have no known competing financial interests or personal relationships that could have appeared to influence the work reported in this paper.

Acknowledgement

The technical guidance of Professor Jihui Tang at the School of Pharmacy, Anhui Medical University is gratefully acknowledged.

Funding

The University Synergy Innovation Program of Anhui Province (GXXT-2020-062); Foundation for the Top Talents in university of Anhui Province (gxbjZD2022013); Scientific Research Promotion Plan of Anhui Medical University (2022xkjT009).

Authors' contributions

JG and QZ conceived and designed the experiments. QZ and SH performed the experiments, analyzed the data and drafted the manuscript. SX, DM and MF analyzed and interpreted the data. JG and QZ confirmed the authenticity of all the raw data. All the authors reviewed the results and read and approved the final version of the manuscript.

References

Al-Majed, A.A., 2009. A direct HPLC method for the resolution and quantitation of the R-(-)- and S-(+)-enantiomers of vigabatrin (gamma-vinyl-GABA) in pharmaceutical dosage forms using teicoplanin aglycone chiral stationary phase. J. Pharm. Biomed. Anal. 50 (1), 96–99. https://doi.org/10.1016/j.jpba.2009.03.030.

Bachmann, D., Ritz, R., Wad, N., Haefeli, W.E., 1996. Vigabatrin dosing during haemodialysis. Seizure 5 (3), 239–242. https://doi.org/10.1016/s1059-1311(96)80043-4.

Ben-Menachem, E., 2011. Mechanism of action of vigabatrin: correcting misperceptions. Acta Neurol. Scand. Suppl. 192, 5–15. https://doi.org/10.1111/j.1600-0404.2011.01596.x.

Bonini, F., McGonigal, A., Trébuchon, A., Gavaret, M., Bartolomei, F., Giusiano, B., et al., 2014. Frontal lobe seizures: from clinical semiology to localization. Epilepsia 55 (2), 264–277. https://doi.org/10.1111/epi.12490.

Buncic, J.R., Westall, C.A., Panton, C.M., Munn, J.R., MacKeen, L.D., Logan, W.J., 2004. Characteristic retinal atrophy with secondary "inverse" optic atrophy identifies vigabatrin toxicity in children. Ophthalmology 111 (10), 1935–1942. https://doi.org/10.1016/j.ophtha.2004.03.036.

Chalasani, N., Bonkovsky, H.L., Fontana, R., Lee, W., Stolz, A., Talwalkar, J., et al., 2015. Features and outcomes of 899 patients with drug-induced liver injury: The DILIN prospective study. Gastroenterology 148 (7), 1340–1352.e1347. https://doi.org/10.1053/j.gastro.2015.03.006.

Čižmáriková, R., Čižmárik, J., Valentová, J., Habala, L., Markuliak, M., 2020. Chiral aspects of local anesthetics. Molecules (Basel, Switzerland) 25 (12). https://doi.org/10.3390/molecules25122738.

Duhamel, P., Ounissi, M., Le Saux, T., Bienayme, H., Chiron, C., Jullien, V., 2017. Determination of the R(-) and S(+)-enantiomers of vigabatrin in human plasma by ultra-high-performance liquid chromatography and tandem mass-spectrometry. J. Chromatogr. B Anal. Technol. Biomed. Life Sci. 1070, 31–36. https://doi.org/10.1016/j.jchromb.2017.10.037.

Durham, S.L., Hoke, J.F., Chen, T.M., 1993. Pharmacokinetics and metabolism of vigabatrin following a single oral dose of [14C]vigabatrin in healthy male volunteers. Drug Metab. Dispos. 21 (3), 480–484.

Elger, C.E., Schmidt, D., 2008. Modern management of epilepsy: a practical approach. Epilepsy Behav. : E&B 12 (4), 501–539. https://doi.org/10.1016/j.yebeh.2008.01.003.

Elwes, R.D., Binnie, C.D., 1996. Clinical pharmacokinetics of newer antiepileptic drugs. Lamotrigine, vigabatrin, gabapentin and oxcarbazepine. Clin. Pharmacokinet. 30 (6), 403–415. https://doi.org/10.2165/00003088-199630060-00001.

French, J.A., Mosier, M., Walker, S., Sommerville, K., Sussman, N., 1996. A double-blind, placebo-controlled study of vigabatrin three g/day in patients with uncontrolled complex partial seizures. Vigabatrin Protocol 024 Investigative Cohort. Neurology 46 (1), 54–61. https://doi.org/10.1212/wnl.46.1.54.

Gale K. Role of GABA in the genesis of chemoconvulsant seizures. Toxicology letters. 1992;64-65 Spec No:417-428.Doi: 10.1016/0378-4274(92)90215-6.

Gibson, J.P., Yarrington, J.T., Loudy, D.E., Gerbig, C.G., Hurst, G.H., Newberne, J.W., 1990. Chronic toxicity studies with vigabatrin, a GABA-transaminase inhibitor. Toxicol. Pathol. 18 (2), 225–238. https://doi.org/10.1177/019262339001800201.

Golec, W., Sołowiej, E., Strzelecka, J., Jurkiewicz, E., Jóźwiak, S., 2021. Vigabatrin - new data on indications and safety in paediatric epilepsy. Neurol. Neurochir. Pol. 55 (5), 429–439. https://doi.org/10.5603/PJNNS.a2021.0063.

Golyala, A., Kwan, P., 2017. Drug development for refractory epilepsy: The past 25 years and beyond. Seizure 44, 147–156. https://doi.org/10.1016/j.seizure.2016.11.022.

Haegele, K.D., Schechter, P.J., 1986. Kinetics of the enantiomers of vigabatrin after an oral dose of the racemate or the active S-enantiomer. Clin. Pharmacol. Ther. 40 (5), 581–586. https://doi.org/10.1038/clpt.1986.227.

Hložek, T., Bursová, M., Coufal, P., Čabala, R., 2016. Gabapentin, pregabalin and vigabatrin quantification in human serum by GC-MS after hexyl chloroformate derivatization. J. Anal. Toxicol. 40 (9), 749–753. https://doi.org/10.1093/jat/bkw070.

Huberfeld, G., Blauwblomme, T., Miles, R., 2015. Hippocampus and epilepsy: Findings from human tissues. Rev. Neurol. 171 (3), 236–251. https://doi.org/10.1016/j.neurol.2015.01.563.

Jammoul, F., Degardin, J., Pain, D., Gondouin, P., Simonutti, M., Dubus, E., et al., 2010. Taurine deficiency damages photoreceptors and retinal ganglion cells in vigabatrin-treated neonatal rats. Mol. Cell Neurosci. 43 (4), 414–421. https://doi.org/10.1016/j.mcn.2010.01.008.

Jung, M.J., Lippert, B., Metcalf, B.W., Böhlen, P., Schechter, P.J., 1977. gamma-Vinyl GABA (4-amino-hex-5-enoic acid), a new selective irreversible inhibitor of GABA-T: effects on brain GABA metabolism in mice. J. Neurochem. 29 (5), 797–802. https://doi.org/10.1111/j.1471-4159.1977.tb10721.x.

Kang, T.C., An, S.J., Park, S.K., Hwang, I.K., Bae, J.C., Won, M.H., 2003. Changed vesicular GABA transporter immunoreactivity in the gerbil hippocampus following spontaneous seizure and vigabatrin administration. Neurosci. Lett. 335 (3), 207–211. https://doi.org/10.1016/s0304-3940(02)01166-7.

Kowalski, K.G., 1994. An algorithm for estimating the terminal half-life in pharmacokinetic studies. Comput. Methods Programs Biomed. 42 (2), 119–126. https://doi.org/10.1016/0169-2607(94)90048-5.

Lado, F.A., Laureta, E.C., Moshé, S.L., 2002. Seizure-induced hippocampal damage in the mature and immature brain. Epileptic Disorders : Int. Epilepsy J. Videotape 4 (2), 83–97.

Li, X., Yang, C., Shi, Y., Guan, L., Li, H., Li, S., et al., 2021. Abnormal neuronal damage and inflammation in the hippocampus of kainic acid-induced epilepsy mice. Cell Biochem. Funct. 39 (6), 791–801. https://doi.org/10.1002/cbf.3651.

Locher, C., Zafrani, E.S., Dhumeaux, D., Mallat, A., 2001. Vigabatrin-induced cytolytic hepatitis. Gastroenterol. Clin. Biol. 25 (5), 556–557.

Lortie, A., Chiron, C., Dumas, C., Mumford, J.P., Dulac, O., 1997. Optimizing the indication of vigabatrin in children with refractory epilepsy. J. Child Neurol. 12 (4), 253–259. https://doi.org/10.1177/088307389701200407.

Lu, H., 2007. Stereoselectivity in drug metabolism. Expert Opin. Drug Metab. Toxicol. 3 (2), 149–158. https://doi.org/10.1517/17425255.3.2.149.

Lux, A.L., Edwards, S.W., Hancock, E., Johnson, A.L., Kennedy, C.R., Newton, R.W., et al., 2005. The United Kingdom Infantile Spasms Study (UKISS) comparing hormone treatment with vigabatrin on developmental and epilepsy outcomes to age 14 months: a multicentre randomised trial. Lancet Neurol. 4 (11), 712–717. https://doi.org/10.1016/s1474-4422(05)70199-x.

Maggiani, G.S.G., Bo, M., 2022. Review of antiseizure medications for adults with epilepsy. JAMA 328 (7), 680. https://doi.org/10.1001/jama.2022.10597.

Mwamwitwa, K.W., Kaibere, R.M., Fimbo, A.M., Sabitii, W., Ntinginya, N.E., Mmbaga, B. T., et al., 2020. A retrospective cross-sectional study to determine chirality status of registered medicines in Tanzania. Sci. Rep. 10 (1), 17834. https://doi.org/10.1038/s41598-020-74932-x.

Nagarajan, L., Schramm, T., Appleton, D.B., Burke, C.J., Eadie, M.J., 1993. Plasma vigabatrin enantiomer ratios in adults and children. Clin. Exp. Neurol. 30, 127–136.

O'Callaghan, F.J., Edwards, S.W., Alber, F.D., Hancock, E., Johnson, A.L., Kennedy, C.R., et al., 2017. Safety and effectiveness of hormonal treatment versus hormonal treatment with vigabatrin for infantile spasms (ICISS): a randomised, multicentre, open-label trial. Lancet Neurol. 16 (1), 33–42. https://doi.org/10.1016/s1474-4422(16)30294-0.

Patsalos, P.N., 2013. Drug interactions with the newer antiepileptic drugs (AEDs)–Part 2: pharmacokinetic and pharmacodynamic interactions between AEDs and drugs used to treat non-epilepsy disorders. Clin. Pharmacokinet. 52 (12), 1045–1061. https://doi.org/10.1007/s40262-013-0088-z.

Rey, E., Pons, G., Richard, M.O., Vauzelle, F., D'Athis, P., Chiron, C., et al., 1990. Pharmacokinetics of the individual enantiomers of vigabatrin (gamma-vinyl GABA) in epileptic children. Br. J. Clin. Pharmacol. 30 (2), 253–257. https://doi.org/10.1111/j.1365-2125.1990.tb03772.x.

Rey, E., Pons, G., Olive, G., 1992. Vigabatrin. Clin. Pharmacokinet. 23 (4), 267–278. https://doi.org/10.2165/00003088-199223040-00003.

Rho, J.M., Boison, D., 2022. The metabolic basis of epilepsy. Nat. Rev. Neurol. 18 (6), 333–347. https://doi.org/10.1038/s41582-022-00651-8.

Ruether K, Pung T, Kellner U, Schmitz B, Hartmann C, Seeliger M. Electrophysiologic evaluation of a patient with peripheral visual field contraction associated with vigabatrin. Archives of ophthalmology (Chicago, Ill : 1960). 1998;116(6):817-819.

Schwarz, M.D., Li, M., Tsao, J., Zhou, R., Wu, Y.W., Sankar, R., et al., 2016. A lack of clinically apparent vision loss among patients treated with vigabatrin with infantile spasms: The UCLA experience. Epilepsy Behav. : E&B 57 (Pt A), 29–33. https://doi.org/10.1016/j.yebeh.2016.01.012.

Scotcher, D., Jones, C., Rostami-Hodjegan, A., Galetin, A., 2016. Novel minimal physiologically-based model for the prediction of passive tubular reabsorption and renal excretion clearance. Eur. J. Pharm. Sci. 94, 59–71. https://doi.org/10.1016/j.ejps.2016.03.018.

Sears, S.M., Hewett, S.J., 2021. Influence of glutamate and GABA transport on brain excitatory/inhibitory balance. Exp. Biol. Med. (Maywood) 246 (9), 1069–1083. https://doi.org/10.1177/1535370221989263.

Sills, G.J., Rogawski, M.A., 2020. Mechanisms of action of currently used antiseizure drugs. Neuropharmacology 168, 107966. https://doi.org/10.1016/j.neuropharm.2020.107966.

Slezia, A., Proctor, C.M., Kaszas, A., Malliaras, G.G., Williamson, A., 2019. Electrophoretic delivery of γ-aminobutyric acid (GABA) into epileptic focus prevents seizures in mice. J. Visual. Exp. : Jove 147. https://doi.org/10.3791/59268.

Sousa, K., Decker, N., Pires, T.R., Papke, D.K., Coelho, V.R., Pflüger, P., et al., 2017. Neurobehavioral effects of vigabatrin and its ability to induce DNA damage in brain cells after acute treatment in rats. Psychopharmacology (Berl.) 234 (1), 129–136. https://doi.org/10.1007/s00213-016-4446-z.

Testa, B., 2015. Types of stereoselectivity in drug metabolism: a heuristic approach. Drug Metab. Rev. 47 (2), 239–251. https://doi.org/10.3109/03602532.2014.984814.

Thijs, R.D., Surges, R., O'Brien, T.J., Sander, J.W., 2019. Epilepsy in adults. Lancet (London, England) 393 (10172), 689–701. https://doi.org/10.1016/s0140-6736(18)32596-0.

Tong, X., Ratnaraj, N., Patsalos, P.N., 2007. The pharmacokinetics of vigabatrin in rat blood and cerebrospinal fluid. Seizure 16 (1), 43–49. https://doi.org/10.1016/j.seizure.2006.10.003.

Valdizán, E.M., García, A.P., Armijo, J.A., 1999. Time course of the GABAergic effects of vigabatrin: is the time course of brain GABA related to platelet GABA-transaminase inhibition? Epilepsia 40 (8), 1062–1069. https://doi.org/10.1111/j.1528-1157.1999.tb00820.x.

Vardi, N., Zhang, L.L., Payne, J.A., Sterling, P., 2000. Evidence that different cation chloride cotransporters in retinal neurons allow opposite responses to GABA. J. Neurosci. 20 (20), 7657–7663. https://doi.org/10.1523/jneurosci.20-20-07657.2000.

Vermeij, T.A., Edelbroek, P.M., 1998. High-performance liquid chromatographic analysis of vigabatrin enantiomers in human serum by precolumn derivatization with o-phthaldialdehyde-N-acetyl-L-cysteine and fluorescence detection. J. Chromatogr. B Biomed. Sci. Appl. 716 (1–2), 233–238. https://doi.org/10.1016/s0378-4347(98)00269-2.

Vigabatrin. LiverTox: Clinical and Research Information on Drug-Induced Liver Injury. Bethesda (MD): National Institute of Diabetes and Digestive and Kidney Diseases; 2012.

Walters, D.C., Jansen, E.E.W., Ainslie, G.R., Salomons, G.S., Brown, M.N., Schmidt, M.A., et al., 2019. Preclinical tissue distribution and metabolic correlations of vigabatrin, an antiepileptic drug associated with potential use-limiting visual field defects. Pharmacol. Res. Perspect. 7 (1), e00456. https://doi.org/10.1002/prp2.456.

Walters, D.C., Jansen, E.E.W., Salomons, G.S., Arning, E., Ashcraft, P., Bottiglieri, T., et al., 2021. Preferential accumulation of the active S-(+) isomer in murine retina highlights novel mechanisms of vigabatrin-associated retinal toxicity. Epilepsy Res. 170, 106536 https://doi.org/10.1016/j.eplepsyres.2020.106536.

Wang, J.H., Hu, S.H., Su, J.Y., Pan, J.P., Mi, X.N., Geng, H.J., et al., 2019. Determination of the pharmacokinetics and tissue distribution of methyl 3,4-dihydroxybenzoate (MDHB) in mice using liquid chromatography-tandem mass spectrometry. Eur. J. Drug Metab. Pharmacokinet. 44 (2), 237–249. https://doi.org/10.1007/s13318-018-0512-8.

Wild, J.M., Robson, C.R., Jones, A.L., Cunliffe, I.A., Smith, P.E., 2006. Detecting vigabatrin toxicity by imaging of the retinal nerve fiber layer. Invest. Ophthalmol. Vis. Sci. 47 (3), 917–924. https://doi.org/10.1167/iovs.05-0854.

Yang, J., Naumann, M.C., Tsai, Y.T., Tosi, J., Erol, D., Lin, C.S., et al., 2012. Vigabatrin-induced retinal toxicity is partially mediated by signaling in rod and cone photoreceptors. PLoS One 7 (8), e43889. https://doi.org/10.1371/journal.pone.0043889.